European Journal of Wood and Wood Products
https://doi.org/10.1007/s00107-024-02123-w

ORIGINAL ARTICLE

Evaluation of wood chips terminal velocity and some morphological properties in a wind tunnel experiment

Gábor Németh[1] · Zoltán Kocsis[1] · Endre Magoss[1]

Received: 11 March 2024 / Accepted: 18 July 2024

Abstract
The removal of wood dust and chips from the work area is also important for occupational health safety regulation and to avoid the risk of fire and dust explosion. Knowledge of the terminal velocity is an important condition for the effective and economical operation of commonly used wood dust-chip extraction systems. While the largest particles are important from the point of view of the operation of the extraction system, knowledge of the terminal velocity of small particles (under 1 mm) is desirable from the point of view of separation and occupational health safety. New measuring and calculation method is developed in order to determine the terminal velocity of wood particles. We built an experimental device to measure the terminal velocity of wood dust-chip particles, and using the experimental results, we modified the calculated terminal velocity based on the modified equivalent particle density (100–130 kg/m^3) in the 1–150 µm size range. The terminal velocity of wood particles under 150 µm more and more deviates from the theoretical values. As a result of mechanical processing, the resulting wood particles' shape is in most cases flat. The average thickness of the wood particles is mainly determined by the sawing parameters. The flat shape of particles increases the specific surface area in a certain extent depending on the distribution parameters.

1 Introduction

Concerning size, shape and density, wood dust and chips may be quite different after mechanical wood processing. Natural particles (sand, crops) are generally smooth, spherical, or ovoid and their density is more or less constant. If crops are comminuted, their surface will be rough, shape irregular and the true density can be determined with difficulties. The most complicated case is a wood particle having very rough surface, irregular shape and its density can hardly be determined due to its internal void structure. For small particles, their size and the size of voids are of the same magnitude.

The wood dust, wood particles under the 500 µm size range can cause different adverse effects on human health. In the wood industry, wood dust is often contaminated with different chemicals (glue, substances of surface treatment) which also causes health risks. Besides nasal adenocarcinoma (Acheson et al. 1981), pathological changes in the lungs of woodworkers have been reported in the past time (Michaels 1967) and certain types of wood are known to produce allergic responses (Hausen 1981). Therefore, both respirable and total dust levels were studied to evaluate health risks arising from wood dust exposures (Shamssain 1992; Lehmann and Fröhlich 1988; Rekhadevi et al. 2008). However, over 0.5 million workers may be exposed to a dust level (any type of wood dust) exceeding 5 mg/m^3. High exposures occur particularly in the construction sector and furniture industry (Kauppinen et al. 2006).

Wood dust is known to be a human carcinogen, based on sufficient evidence of carcinogenicity from studies on humans. It has been demonstrated through human epidemiologic studies that exposure to wood dust increases the occurrence of cancer of the nose (nasal cavities and paranasal sinuses) (NTP Board 2000).

The knowledge of terminal velocity is also important in the dust separation process. In a cyclone, the separation velocity of particles is direct proportional to the terminal velocity. Therefore, the separation efficiency also depends on the terminal velocity. It is well known that the terminal velocity can be calculated for spherical bodies. It works

✉ Gábor Németh
nemeth.gabor@uni-sopron.hu

[1] Faculty of Wood Engineering and Creative Industries, University of Sopron, Bajcsy-ZS. U. 4, Sopron 9400, Hungary

Published online: 05 August 2024

well, for example, with wheat corn. Sadly, it does not work with small wood particles at all. What is the reason? In calculations the gravitational force and drag force are equally important. For small wood particles, first of all, the determination of gravitational force causes the main brain racking. Therefore, only experimental methods are suitable (Magoss et al. 2022).

Wood dust is not only harmful for the human health but also under special boundary conditions wood dust is flammable and explosive material. At the same time wood is one of the most valuable renewable raw materials in the world. Therefore, researchers extensively have investigated the wood cutting theory of different woodworking operations in order to define the particle size distribution of the wood chips and dust (Sitkei 1994; Rautio et al. 2007; Csanády and Magoss 2013; Reisz and Magoss 2013; Ojima 2016). Usually, the smaller particle size fraction could cause the most effect in both cases. Wood dust is an unavoidable by-product of the mechanical wood processing. Exposure to wood dust may occur in all mechanical woodworking operations, but the concentration varies greatly, depending on the distance from the point of operation and whether the worker is operating the saw from an enclosed booth (Teschke et al. 1994). The highest proportion of respirable dust relative to total dust was measured at workplaces with low overall dust exposure and on machines that produce chips with the smallest chip thicknesses (Kos et al. 2004). In general, thermally modified wood has increased fragility and brittleness, which results in the production of smaller dust particles than unmodified wood (Očkajová et al. 2016) The thermal modification treatment has minor effects on the wood particle mass concentration (PM), aerosol size distribution generated when the wood is processed on a typical industrial table saw (Aro et al. 2019). Rattan also produced significantly higher amounts of finer dust than bamboo and wood during mechanical processing, which can seriously affect the respiratory system of workers (Ratnasingam and Scholz 2015).

In order to establish the particle size distribution usually multistage cascade impactor is used. A new method is introduced to evaluate the particle sizes and size distribution, the use of Scanning Electron Microscopy (SEM) and image processing program. The method is accurate, quick and reproducible (Mazzoli and Favoni 2012).

Some studies reported that the particle size distribution varied according to the woodworking operation, with sanding producing smaller particles than sawing (Hounam and Williams 1974; Darcy 1984; Wu and Liu 1985; all cited in IARC 1995), but others found no consistent differences (Holliday et al. 1986; Lehmann and Fröhlich 1988; and Pisaniello et al. 1991; all cited in IARC 1995). Much of the wood dust mass was reported to be contributed by particles larger than 10 µm in aerodynamic diameter (Whitehead et al. 1981; Darcy 1984; Lehmann and Fröhlich 1988; Hinds 1988; and Pisaniello et al. 1991; all cited in IARC 1995). Holliday et al. 1986; cited in IARC 1995) found that 61–65% of the particles measured are between 1 and 5 µm in diameter.

Small wood particle with 10 µm diameter loses its initial velocity faster than the particle with 100 µm diameter. Therefore, small particles require additional air motion to get them safely into the collecting tube (Magoss et al. 2022).

Wood dust is also part of the biomass, which is currently used as an alternative fuel such as renewable energy sources. Experts assess the potential concerns associated with the use of biomass fuels when combusted in terms of health and safety as well as the risk of explosion (Marková et al. 2016). However, wood dust is flammable and will ignite in the environment. It may present a strong to severe explosion hazard if a dust cloud contacts an ignition source. Wood dust is stable under normal laboratory conditions. The literature provided no information about decomposition in the environment. Studies show that particle morphology impacts dust cloud minimum ignition energy (MIE) via heat transfer because higher specific surface results in lower conductive heat resistance. However, heat transfer is not the only factor impacting MIE; the effect of particle morphology on cloud dynamics is another important factor (Prasad et al. 2021). A calculation method of the wood dust explosion is introduced (Callé et al. 2005). The model based on balances on chemical reaction, kinetics and thermodynamics leads to the representation of the pressure change during the explosion. The experimental results also show that the violence of the explosion is all the more higher as the particle size is low. Addition of ultrafine $Mg(OH)_2$ exerted obvious effects on the flame propagation of wood dust (Huang et al. 2019).

The technology of the wood processing is seldom optimized on the health and fire hazards; therefore, the wood dust emission must be under control through licencing as well as by the use of extraction systems (Husgafvel-Pursiainen 2004). In the practice, using proper dust extraction systems, occupational exposure to wood dust and the biohazards associated with wood dust can be prevented or minimized. When the exposure cannot be fully controlled, workers should be provided with appropriate personal protective equipment. Workers should also be educated on the potential health effects of wood dust exposure (Mandryk et al. 1999). The use of personal protective equipment, general ventilation, etc., is less effective, because it eliminates the effects of dust dispersion. It is therefore necessary to educate on the principles of design and operation of dust exhaust systems in the wood industry, in order to properly use their capabilities (Pałubicki et al. 2020).

The energy consumption of the dust extraction system could be very high level depending on the air velocity of the pipeline. In order to optimize the electric energy consumption of the extraction system the terminal velocity of the biggest wood particles of the system must be known. The terminal velocity is not fully investigated in the wood science but in the literature some experiment results can be found for different materials (Wheatley 1951; Timbrell 1954; Beard 1976; Zhang et al. 2014; Fadzír et al. 2020; Zhou et al. 2021; Kalman and Matana 2022). Therefore, the terminal velocity of the wood particles is very important in order to optimize the working parameters of the extraction systems.

In the literature, the determination of the terminal velocity has not excessively been investigated, especially concerning the wood particles. The reason for it is the following. Accurate measurement and evaluation could have been done only with uniform particles, the production of which is practically impossible. Using a given fraction with its own particle size distribution creates many difficulties and uncertainties in the evaluation of measurement results. Namely, the accurate correspondence between particle size and floating velocity can hardly be ensured.

The aerodynamic drag of peat particles of various sizes in an air flow was studied, and a criterion relationship between the drag coefficient (CD) and the Reynolds number (R_e) was determined (Evdomikov et al. 2020). Accurate design charts for CD were prepared and displayed for all particle sphericities (Haider and Levenspiel 1989). A concise and straightforward way for calculating the Reynolds number, the drag coefficient and the terminal velocity of pumices is available to modellers for better constraining parameters in numerical simulation codes and implementing hazard scenarios with better quality data (Dellino et al. 2005).

The most important aspects of the terminal velocity in the wood industry are the following: health hazards, fire and dust explosion hazards, particle separation and electric energy consumption of the extraction systems.

In principle, the terminal velocity problem is clear and simple: the weight force of a particle is in equilibrium with the aerodynamic drag force of the fluid. In practice, however, we have a lot of difficulties and uncertainties. The reason for it is that we have particles with irregular shape and rough surface, and with internal voids of random distribution. Furthermore, we cannot handle a single small particle in our experiments, but only a small amount of bulk particles taken from a given fraction of particles. Therefore, we can calculate only with average values. The average diameter related to the particle surface is, however, by far not the same as that related to the particle weight (Magoss et al. 2022) .

Table 1 Operational parameters of the table saw machine

Machine type	Cutting speed	Feed speed	Feed per tooth	Depth of cut
Table saw	55 m/sec	6 m/min	0.2 mm	25 mm

Table 2 Average moisture content of the samples

	Average moisture content (%)
Poplar/table saw	8.50
Norway spruce /table saw	9.58
Beech/table saw	9.13

We are more lucky with the Reynolds number of the medium. In a cyclone, the Reynolds number varies at least between 10^4 and 10^5. In our measuring tube, there are values from 3400 to 8000. Earlier drag force measurements for regular shapes show that the drag coefficient for Reynolds numbers between 10^3 and 10^5 can be taken as constant, but the true drag coefficient for our average shape and size with boundary layer is a big question.

Our aim is to contribute to these hardly transparent problems, in particular with respect to shape and size in different fractions, the possible surface increment related to regular shape, to give some data for the apparent density for fractions, and measured terminal velocities for fractions.

2 Materials and methods

In the experiment, three types of wood species were examined. The species studied were poplar (*Populus tremula*), Norway spruce (*Picea abies*) and beech (*Fagus sylvatica*). During the longitudinal sawing of the chips and dust samples, sawdust samples were collected in a bag of a mobile extractor placed at the pre-cleaned sawdust discharge section of the circular saw machine. To conduct a reliable sieve analysis, the sample bag was thoroughly shaken (homogenized) before sieving, according to the requirements of the MSZ EN 14778 standard, and then sampling was performed from the top, middle, and bottom to obtain representative results. The sieving was conducted according to the relevant standard (MSZ EN ISO 17827-2:2016) guidelines, with particular attention to ensuring that the test sample weighed at least 50 g and that the layer thickness on the upper sieve did not exceed 2 cm.

Tables 1 and 2 show the wood cutting parameters and the moisture content of the samples respectively. The moisture content of the samples was measured using a Kern DLB160-3 A wood moisture meter.

Particle size distribution was determined with a type CISA BA 200 N multistage cascade impactor. The impactor separates the particles by mass, allowing dust collected at various stages to be weighed and a particle size (mass) distribution to be determined according the MSZ EN ISO

17827-2:2016 norm. The mesh sizes of the subsequent sieves were the following: 1 mm, 0.8 mm, 0.5 mm, 0.2 mm, 0.063 mm, and the dummy receiver for particles less than 0.063 mm. For weighing, the screen residue was measured by a Kern PCB 3500-2 analytic scale.

The sieve analysis was repeated three times for each wood species. The average mass of the samples was 96.91 g with a standard deviation of ± 3.5 g.

Knowing the single screen residue, their relative values were determined in percent:

$$m_{fr\%} = \frac{m_{fr}}{m_{sample}} \cdot 100 \quad (1)$$

The cumulated value of the single screen residues gives the sieve residue curve as a function of particle diameter. The size distribution curve of wood particles is always asymmetric; therefore, a suitable theoretical distribution curve should be selected. Long-time experience has shown that the use of logarithmic normal distribution function gives good approximation with the further advantage that its mathematical treatment is easy (Sitkei 1994; Reisz and Magoss 2013).

To determine the surface area of different fractions, we used 30 grains per fraction using a DELTE Optical Smart 5MP Pro digital microscope. The images of the samples were processed, and the surfaces determined using the image analysis and size/surface determination module of Photoshop software. Correct calibration of the scale was assisted by the 1 mm calibration dimensions on the sample table (Fig. 1).

There are oblong particles giving higher surface area than that of the corresponding mesh size.

A measurement error cannot be determined by itself, so it is necessary to determine the uncertainty of the measurement procedure. As a result of multiple surface measurements of the same grain, it can be established that the value of the measurement uncertainty (relative standard deviation of the measurement results) of each surface is 0.7%. This is not the same as that calculated from the standard deviation of the set of 30 samples taken from the given fraction, which depends to a large extent on the fractions and the shape of the wood particles, so it also varies greatly based on our measurements, but on average it is between 5 and 10%.

To define the thickness of the dust particles also is a difficult measuring problem. The shape of the dust particles is versatile and usually curved. Therefore, we applied light pressure on the particles during the measuring process to flatten them out. A Marcator 1087 micrometer was used, so the spindle was suitable for performing the smoothing task too (Fig. 2).

Fig. 1 Calibration of the optical measuring system

Fig. 2 Smoothing effect of the micrometer's spindle

To determine the terminal velocity of the different size ranges of the samples a new measuring device was designed and built (Fig. 3).

To control the air volume and air velocity, a radial fan with a frequency converter was used, and an anemometer showed the air velocity. The first step in measuring the terminal velocity of the wood particle is loading it onto the sample catch sieve. The air velocity must be increased until the wood particle hovers in the air. The equilibrium state between the air drag force and the gravitational force results in the terminal velocity. The process is visually observable through the Plexiglas pipe section (floating section). The

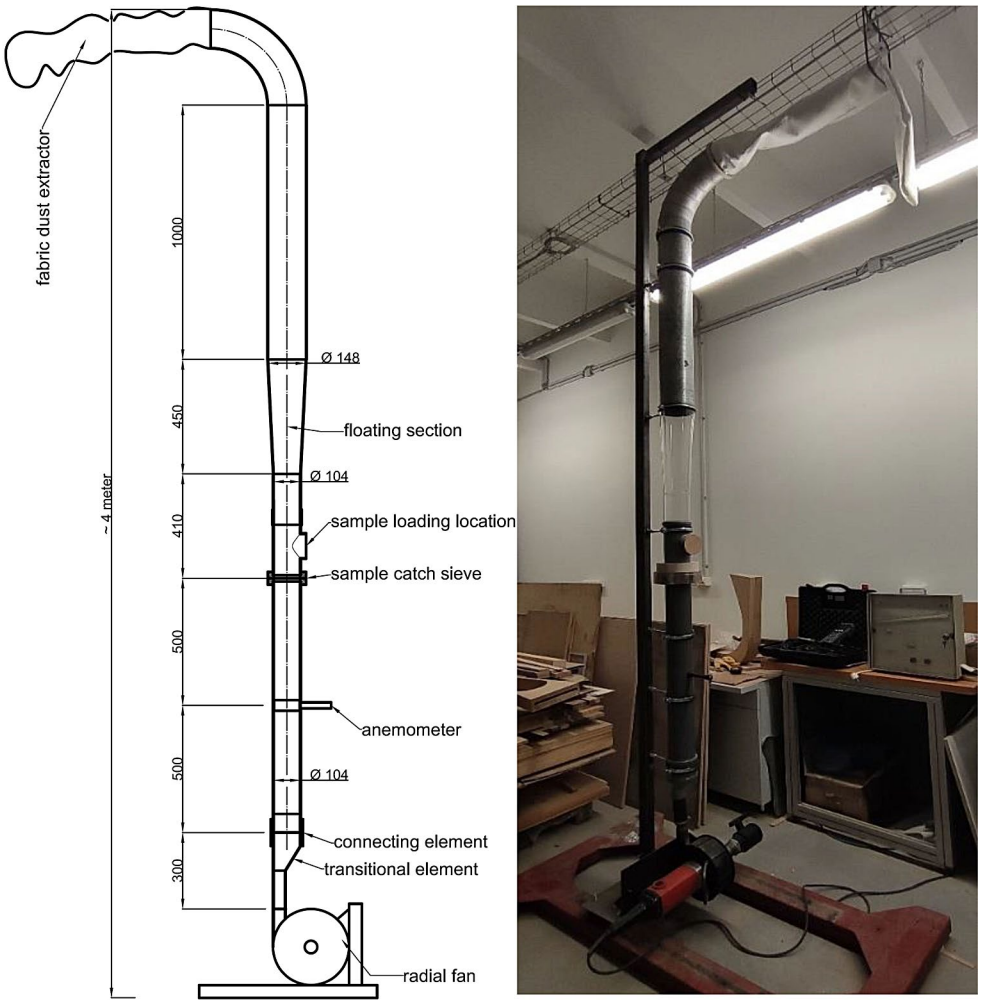

Fig. 3 Special measuring system to determine the terminal velocity of the wood particles

minimum flow velocity in the measuring section is 0.15 m/s at which $Re = 10^3$ and the drag coefficient is independent of flow velocity.

To produce small particles of constant size is practically impossible, and we are forced to use a given fraction with its own particle size distribution. In order to have a more accurate reading and evaluation, the following measurement procedure was used. The air flow velocity was very slowly increased and, observing the first floating particles, the corresponding velocity was read. As the air velocity was further increased, more and more particles were floating according to the distribution of the fraction used. As air velocities further increased, the number of floating particles decreased due to the smaller quantity of bigger particles in the fraction.

Operational safety of the wood dust/chips extraction systems requires to lift the biggest/heaviest wood particle and at the same time the air velocity of the pipeline basically influences the electric energy consumption of the extraction system. Therefore, the terminal velocity is a fundamental design parameter. The tiniest wood particles become easily airborne, and its settling process is slow in the workroom, therefore the wood dust could cause occupational hazard for the workers. In order to deeper understand the correlation of the particle size and its terminal velocity, our experiment covered the whole size range of the samples.

In order to constantly check the values of drag coefficients, the apparent density of dust particles for the different fractions is also needed. We used a direct measurement method using a scale of 0.1 mg accuracy and the number of particles was counted. Generally, 50 mg dust was dispersed on the scale table and the number of particles varied between 400 and 700. The obtained value may be regarded as the upper limit of density due to the adherence of finer particles to the bigger ones.

3 Results and discussion

Using the common sieve analysis, the experimental results are plotted in a probability diagram (Fig. 4). In order to obtain the particle size distribution curve as straight line,

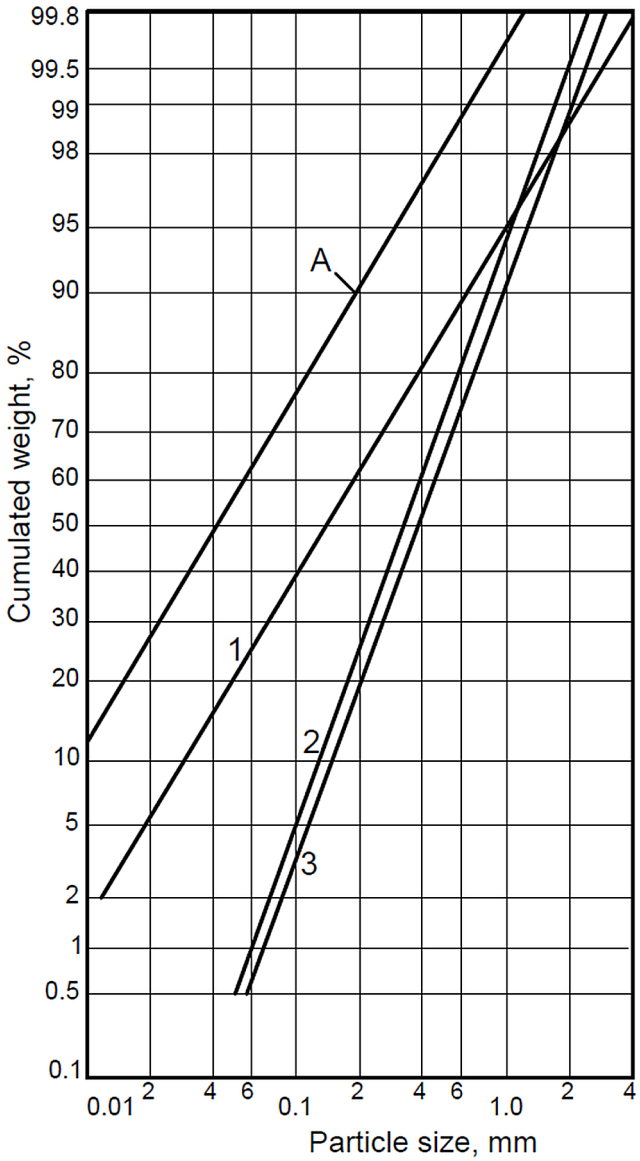

Fig. 4 Cumulated probability function of particles for different wood species. The distribution of specific surface area (A) is also provided for curve 1 (1 – beech table saw; 2 – poplar table saw; 3 – spruce table saw)

we have used probability net. The work with this type of curve is easier. As can be seen, there are no significant differences between the samples of the three wood species produced by table circular saw machine. In the case of beech, it can be seen that the particle size describes a wider size range (0.01–4 mm), compared to spruce and poplar samples (0.05–3 mm). The poplar and spruce samples gave almost the same results (curves 2 and 3). For the table circular saw, the size range above 1 mm is not relevant, so it is not included in the analysis. The next stage of our research will focus on the wood planing process, i.e. detailed analysis of the larger size range of the particle size distribution.

Table 3 shows the calculated distribution parameters for the tested wood species, including their specific surface area.

The distribution function is given by the following equation:

$$y = \frac{1}{\sqrt{2\pi} \cdot \overline{X} \cdot \sigma \cdot e^{\sigma^2/2}} \cdot e^{-\left(ln\left(x/\overline{X}\right)\right)^2/2\sigma^2} \quad (2)$$

where.

M_i – is the median (is the diameter to 50%);

QR – is the quarter ratio ($QR = \frac{X_3 - Mi}{Mi - X_1}$, where: x_3 – is the diameter to 75%; x_1 – is the diameter to 25%);

σ – is the standard deviation ($\sigma = 1.481 \cdot ln(QR)$);

$\overline{X}$ – is the mode ($\overline{X} = Mo = Mi \cdot e^{-\sigma^2}$);

X_{av} – is the geometric mean ($X_{av} = \overline{X} \cdot e^{1.5 \cdot \sigma^2}$);

A – is the specific particle surface area.

In the next step, we determine the geometric dimensions of the particles in all the size ranges defined by the sieve analysis. In each size range, the size of 30 randomly selected particles was measured, from which the average surface and average thickness values were determined (Table 4).

The average thickness values are more or less constant for all fractions. That means that the thickness is mainly determined by the cutting parameters.

For further characterization of particle shape, a simple sphericity index (SI) was defined in the following form. Using the measured surface area, we can calculate the area-based equivalent diameter

$$d_A = \sqrt{\frac{4 \cdot A_i}{\pi}} \quad (3)$$

where A_i - is the measured surface area for a given fraction, mm^2.

An approximate particle volume is given by multiplying the surface area with the particle thickness. As before, we can calculate a volume-based equivalent diameter

Table 3 Main characteristics of the distribution curves given in Fig. 4

No.	Mi (mm)	QR	σ	$\overline{X}$ =Mo (mm)	X_{av} (mm)	A (m^2/kg)
1.	0.14	2.21	1.18	0.04	0.28	415
2.	0.33	1.72	0.80	0.17	0.46	100
3.	0.38	1.65	0.74	0.22	0.51	95

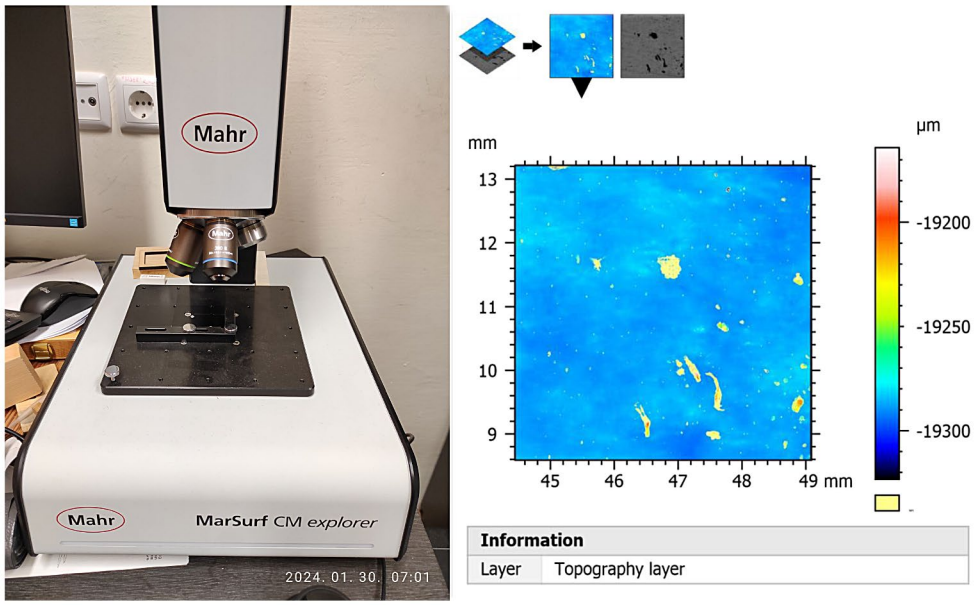

Fig. 5 MarSurf CM explorer type optical measuring system (measurement uncertainty within the applied measurement range +/- 0.050 µm)

Table 4 Shape characterization

Fraction, (mm)	Average surface area (mm^2)	Standard deviation	Average particle thickness, (mm)	Standard deviation	Area-based equivalent diameter d_A (mm)	Volume-based equivalent diameter d_V (mm)	SI
Spruce - circular saw							
1-0.8	1.1532	0.3102	0.0729	0.0186	1.2120	0.5436	0.4485
0.8 – 0.5	0.7176	0.2833	0.1046	0.0159	0.9561	0.5235	0.5475
0.5 – 0.2	0.2593	0.1251	0.0868	0.0141	0.5747	0.3504	0.6096
*0.2-0.063**	0.1654	-	0.0256	-	0.4590	0.2008	0.4374
Poplar - circular saw							
1-0.8	1.2988	0.3493	0.0750	0.0180	1.2863	0.5710	0.4439
0.8 – 0.5	0.5464	0.1813	0.0981	0.0093	0.8343	0.4679	0.5608
0.5 – 0.2	0.2715	0.1420	0.0629	0.0109	0.5881	0.3196	0.5434
*0.2-0.063**	0.1885	-	0.0208	-	0.4900	0.1957	0.3993
Beech - circular saw							
1-0.8	1.3949	0.6016	0.1360	0.0290	1.3330	0.7130	0.5349
0.8 – 0.5	0.6710	0.3151	0.0446	0.0114	0.9245	0.3853	0.4167
0.5 – 0.2	0.2419	0.0961	0.0386	0.0060	0.5551	0.2613	0.4707
*0.2-0.063**	0.1747	-	0.0185	-	0.4717	0.1835	0.3889

*Our measuring method to define the particle thickness in the size range 0.2–0.063 mm is difficult to carry out. The small wood particles do not tend to curve, therefore, an optical measuring system (Fig. 5) was used to measure the thickness of these particles

$$d_V = \sqrt[3]{\frac{6 \cdot V_i}{\pi}} \tag{4}$$

where V_i - is the average volume of particles in a given fraction, mm^3.

The sphericity index is the ratio of the above average diameters

$$SI = \frac{d_V}{d_A} \tag{5}$$

For a sphere, SI is equal to one.

As mentioned earlier, no reliable data are available for drag coefficients of fine dust particles with irregular shape and rough surface. In order to calculate drag coefficient, the apparent density of particles is needed. Using a simple weighing method, we measured one fraction and three wood species. The results are summarized in Table 5.

Table 5 shows that the apparent density of the fraction (based on specific weight of particle) ranging from 0.8 to 1.0 mm varies between 0.14 and 0.22 g/cm^3 and does not

Table 5 Specific weight of particle

Species	Mass (mg)	Number in sample	Specific weight of particle (γ_m), (N/m^3)	Calculated terminal velocity (v_{cr}), (m/s)
Spruce	50	609	2122	1.03
Poplar	50	611	2092	1.05
Beech	50	650	1469	0.98

follow exactly the volume weight of the species. For smaller fractions, the apparent density slightly decreases.

The terminal velocity was calculated with Eq. (6). The selection of drag coefficient requires some considerations. We have seen earlier that the examined saw dust contains a considerable amount of flat shapes. The drag coefficient for flat disc with smooth surface has a value of 1.1. The saw dust particles have a rough surface and the roughness heights are mostly higher than the boundary layer thickness. That means that, with all probability, additional friction resistance occurs. Therefore, drag coefficients with values around 1.2 may be predicted. It should be remembered that the investigations of Nikuradze (1930) for tube resistance support the considerable effect of roughness on the friction resistance.

The calculated terminal velocities are the upper limit of measured values. Therefore, we believe that measured and calculated terminal velocities are in good agreement and represent a good approximation for the given fraction. The terminal velocity for sphere is calculated as:

$$v_{cr} = \sqrt{\frac{4 \cdot d_v \cdot \gamma_{m \cdot g}}{3 \cdot c_e \cdot \gamma_a}} \tag{6}$$

where c_e – is the drag coefficient (during the calculations, we assumed a value of c_e=1.2);

γ_m – is the specific weight of particles, N/m^3;

γ_a – is the specific weight of air, N/m^3.

Unfortunately, wood dust particles are of irregular shape with rough surfaces and their drag coefficients depend on the instantaneous position (orientation). Assuming regular shapes, we can specify some upper and lower limit values. The sphere has a value of c_e=0.44 and the flat disc c_e=1.1. Considering our measurement results for particle shapes, it may be concluded that the considerable amount of flat particles gives grounds for taking higher drag coefficient. Furthermore, if we take into consideration the presence of rough surfaces with higher friction forces, we may take a drag coefficient of 1.2. We have now reliable data for particle density, therefore, the theoretical calculations for terminal velocities can be compared with the measured values with acceptable accuracy.

Table 6 and Fig. 6 show the experimental results. The calculated terminal velocities are referred to the average size of each fraction.

If we consider the possible uncertainties of the measurement readings within a given fraction, the agreement is fully acceptable. This result supports the validity of a relatively high drag coefficient due to the flatter shape and rough surface.

For comparison, our earlier experimental results with three wood species are included which do not differ much from the present values (Fig. 7) (Magoss et al. 2022).

The course of variation follows the theoretical line down to some 150 µm, but the recalculated equivalent particle density (100–130 kg/m^3) is much less than the density of solid wood (Fig. 7). For smaller particles, however, the

Table 6 Measured and calculated terminal velocities

Fraction, (mm)	Minimum air velocity (the particle are lifted by the air current), (m/s)	Maximum air velocity (the air current carries the particles away), (m/s)	Average particle volume (V), (mm^3)	Specific weight of particle (γ_m), (N/m^3)	Calculated terminal velocity (v_{cr}), (m/s)
Spruce - circular saw					
1-0.8	1.15	2.59	0.0841	2122	1.03
0.8 – 0.5	0.86	2.54	0.0751	2141	1.02
0.5 – 0.2	0.78	2.21	0.0225	2271	0.86
0.2-0.063	0.57	1.86	0.0042	2346	0.66
Poplar - circular saw					
1-0.8	1.06	2.38	0.0974	2092	1.05
0.8 – 0.5	0.91	2.10	0.0536	2195	0.97
0.5 – 0.2	0.68	1.85	0.0171	2840	0.91
0.2-0.063	0.53	1.65	0.0039	2965	0.73
Beech - circular saw					
1-0.8	0.94	2.17	0.1897	1469	0.98
0.8 – 0.5	0.78	2.07	0.0299	1510	0.73
0.5 – 0.2	0.72	1.94	0.0093	2437	0.77
0.2-0.063	0.59	1.72	0.0032	2869	0.70

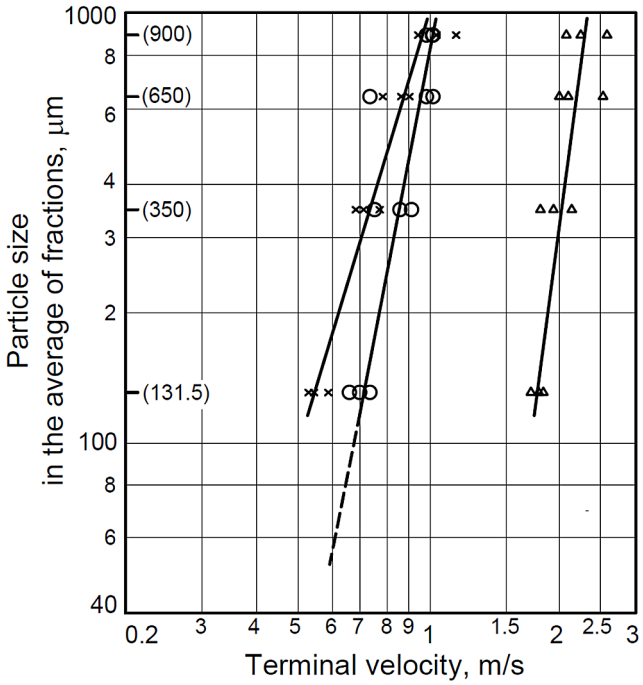

Fig. 6 Graphical representation of the results (X – minimum air velocity; O – calculated terminal velocity; Δ – maximum air velocity)

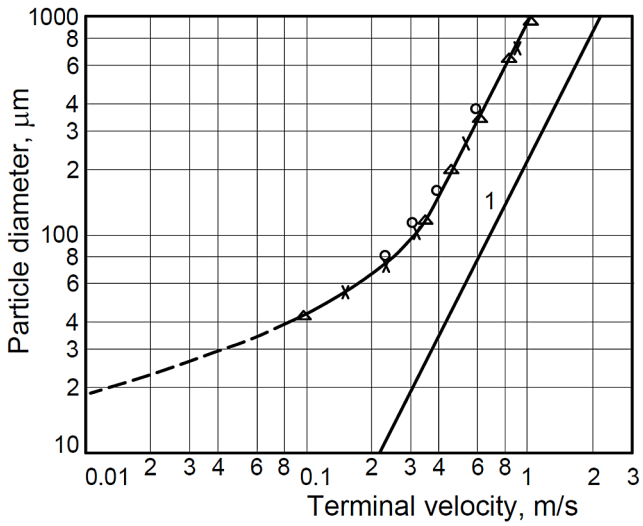

Fig. 7 Terminal velocities measured for narrow dust fractions of pine, beech and oak species and theoretical terminal velocity (1). 1–500 kg/m^3 (Magoss et al. 2022)

deviation rapidly increases. That is the reason that particles around 5 µm diameter can be floating for longer time in resting air. Furthermore, Brownian movement (after Robert Brown 1827) of the air also contributes to the floating of fine particles to a certain extent, due to the high surface per mass ratio.

In the higher size ranges, the shape of particles may become flatter. This means a higher specific surface compared to the theoretical one, which can simply be calculated

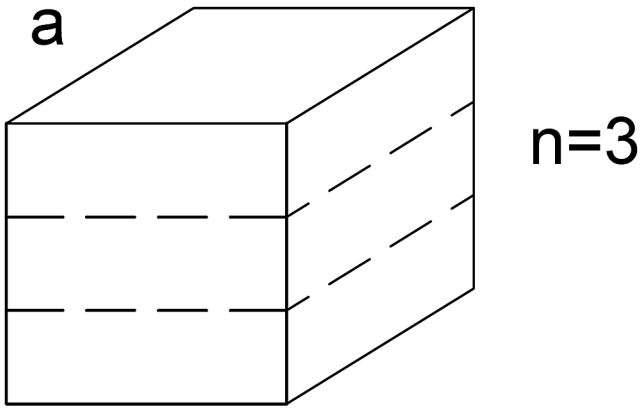

Fig. 8 Modelling of a particle cut into slices

from the distribution parameters (Magoss et al. 2022). The actual surface area is a more difficult task. If we model a particle as a cube which is cut into "*n*" slices (see Fig. 8), then the surface (A) increases as a function of number of slices in the following manner:

$$A = 2 \cdot a^2 \, (2 + n) \, (\mathrm{m}^2) \tag{7}$$

where:

a – is the length of cube edge;

n – is the number of slices.

The surface increment is calculated as.

$$A_{in} = \frac{A_x - A_0}{A_0} = \frac{1}{3} \cdot (n - 1) \; (\%) \tag{8}$$

where.

A_x – is the actual surface within the taken size range and for a given slice number;

A_0 – is the theoretical surface within the same size range, which can be read in Fig. 4.

For example, if $n = 4$, the surface is doubled and the increment is 100% within the given size range, related to the theoretical portion of surface within the same range. The cumulated increments give the total increment related to the whole theoretical surface area as 100%.

A quantitative analysis requires, however, further special measurements and evaluations. At the same time, the theoretical specific surface area given in Table 3, supplies a good orientation, especially for comparison purposes.

4 Conclusion

Based on experimental results and theoretical considerations discussed earlier, the following main conclusions may be drawn:

- These experiments show that a considerable amount of particles may be flat, oblong with rough surface.
- The obtained morphological properties suggest a relatively high drag coefficient with values around 1.2.
- We determined the apparent density of wood particles (0.8–1.0 mm size range) which are 140–220 kg/m^3 These data enable to carry out more accurate calculations for determining terminal velocities.
- In the higher size ranges, the shape of particles may become flatter, causing their behaviour in the air flow differ from that of smaller particles. In the size range of 0.8–1.0 mm, the ratio of the apparent density (140–220 kg/m^3) to the particle density calculated from the measured terminal velocity (100–130 kg/m^3) is almost double. The ratio increases as the particle size decreases.
- Due to the irregular shape of particles, the area-based equivalent diameter and the weight-based one are not the same.
- The measured and calculated terminal velocities are in acceptable agreement.

We naturally aim to continue our research, therefore, we will investigate the relationship between dust-chip mixtures and terminal velocity based on the research method described earlier, also for other woodworking machinery. Woodworking machines and their machining parameters vary significantly, so it is essential to conduct more measurements to reduce occupational health and environmental impacts.

Author contributions Gábor Németh contributed to the methodology, data curation, formal analysis, measurement system design, implementation and investigation. Zoltán Kocsis assisted with measurement system design, implementation, measurement, data analysis, processing and visualization. Endre Magoss was involved in conceptualization, data curation, data analysis, writing review, supervision.

Funding Open access funding provided by University of Sopron.

Data availability No datasets were generated or analysed during the current study.

Declarations

Competing interests The authors declare no competing interests.

References

Acheson ED, Cowdell RH, Rang EH (1981) Nasal cancer in England and Wales: an occupational survey. Occup Environ Med 38(3):218–224

Aro MD, Geerts SM, French S, Cai M (2019) Particle size analysis of airborne wood dust produced from sawing thermally modified wood. Eur J Wood Prod 77(2):211–218

Beard KV (1976) Terminal velocity and shape of cloud and precipitation drops aloft. J Atmos Sci 33(5):851–864

Callé S, Klaba L, Thomas D, Perrin L, Dufaud O (2005) Influence of the size distribution and concentration on wood dust explosion: experiments and reaction modelling. Powder Technol 157(1–3):144–148

Csanády E, Magoss E (2013) Mechanics of wood machining. Springer, Berlin, pp 168–171

Darcy FJ (1984) Woodworking operations: furniture manufacturing. Industrial hygiene aspects of plant operations. Macmillian, Toronto, pp 349–362

Dellino P, Mele D, Bonasia R, Braia G, La Volpe L, Sulpizio R (2005) The analysis of the influence of pumice shape on its terminal velocity. Geophys Res Lett, 32(21)

Evdomikov OA, Mikhailov AS, Veretennikov SV, Serov RA (2020) Experimental determination of the terminal velocity and the Drag Coefficient of Peat Dust particles. Solid Fuel Chem 54(5):299–304

Fadzír AFM, Rani SI, Gimbun J (2020) Dispersion of Irregular Particles during Free Fall. J Phys Conf Ser 1532(1):012010

Haider A, Levenspiel O (1989) Drag coefficient and terminal velocity of spherical and nonspherical particles. Powder Technol 58(1):63–70

Hausen BM (1981) Woods injurious to human health: a manual. W. de Gruyter, pp 189–pp

Hinds WC (1988) Basic for size-selective sampling for wood dust. Appl Industrial Hygiene 3(3):67–72

Holliday SB, Horwich A, Deacon JM, Peckham MJ (1986) A toxicity and pharmacokinetic study in man of the hypoxic-cell radiosensitiser RSU-1069. Br J Radiol 59(708):1238–1240

Hounam RF, Williams J (1974) Levels of airborne dust in furniture making factories in the high Wycombe area. Occup Environ Med 31(1):1–9

Huang C, Chen X, Yuan B, Zhang H, Dai H, He S, Shen S (2019) Suppression of wood dust explosion by ultrafine magnesium hydroxide. J Hazard Mater 378:120–723

Husgafvel-Pursiainen K (2004) Wood dust-related health effects and occupational limit values. In Wood dust symposium 15th, Coppenhagen

Hungarian Standards Institute (2016) MSZ EN ISO 17827-2:2016: Determination of particle size distribution for uncompressed fuels. Part 2: Vibrating screen method using sieves with aperture of 3.15 mm and below (ISO 17827-2:2016. Budapest, Hungary

Hungarian Standards Institute (2011) MSZ EN 14778:2011. Solid biofuels – sampling. Budapest, Hungary

Kalman H, Matana E (2022) Terminal velocity and drag coefficient for spherical particles. Powder Technol 396:181–190

Kauppinen T, Vincent R, Liukkonen T, Grzebyk M, Kauppinen A, Welling I, Savolainen K (2006) Occupational exposure to inhalable wood dust in the member states of the European Union. Ann Occup Hyg 50(6):549–561

Kos A, Beljo-Lučić R, Šega K, Rapp AO (2004) Influence of woodworking machine cutting parameters on the surrounding air dustiness. Holz Roh- Werkst 62(3):169–176

Lehmann E, Fröhlich N (1988) Particle size distribution of wood dust at the workplace. J Aerosol Sci 19(7):1433–1436

Magoss E, Sitkei G, Kocsis Z (2022) Dust extraction and handling in the Wood Industry. Springer Nat P 123. https://doi.org/10.1007/978-3-031-08915-2

Mandryk J, Alwis KU, Hocking AD (1999) Work-related symptoms and dose-response relationships for personal exposures and pulmonary function among woodworkers. Am J Ind Med 35(5):481–490

Marková I, Mračková E, Očkajová A, Ladomerský J (2016) Granulometry of selected wood dust species of dust from orbital sanders. Wood Res 61(6):983–992

Mazzoli A, Favoni O (2012) Particle size, size distribution and morphological evaluation of airborne dust particles of diverse woods by scanning electron microscopy and image processing program. Powder Technol 225:65–71

Meeting of the NTP Board—National Toxicology Program—of Scientific Counselors Report on Carcinogens Subcommittee (2000) Report on carcinogens background document for wood dust. Atlanta, GA: U.S. Department of Health and Human Services, National Institute of Environmental Health Sciences, https://ntp.niehs.nih.gov/sites/default/files/ntp/newhomeroc/roc10/wd_no_appendices_508.pdf

Michaels L (1967) Lung changes in woodworkers. Can Med Assoc J 96(16):1150

Nikuradse J (1930) Widerstandsgesetz Und Geschwindigkeitsverteilung Von turbulenten Wasserströmungen in glatten und rauhen Rohren. (Resistance law and velocity distribution of turbulent water flows in smooth and rough pipes). Verh D 3 Intern Kongr f Techn Mech Stockholm 1930 Stockholm 1931, Bd 1:239

Očkajová A, Kučerka M, Banski A, Rogoziński T (2016) Factors affecting the granularity of wood dust particles. Chip Chipless Woodwork Process 10(1):137–144

Ojima J (2016) Generation rate and particle size distribution of wood dust by handheld sanding operation. J Occup Health 58(6):640–643

Pałubicki B, Hlásková L, Rogoziński T (2020) Influence of exhaust system setup on working zone pollution by dust during sawing of particleboards. Int J Environ Res Public Health 17(10):3626

Pisaniello DL, Connell KE, Muriale L (1991) Wood dust exposure during furniture manufacture—results from an Australian survey and considerations for threshold limit value development. Am Ind Hyg Assoc J 52(11):485–492

Prasad S, Schweizer C, Bagaria P, Kulatilaka WD, Mashuga CV (2021) Effect of particle morphology on dust cloud dynamics. Powder Technol 379:89–95

Ratnasingam J, Scholz F (2015) Dust emission characteristics in the bamboo and rattan furniture manufacturing industries. Eur J Wood Prod 73(4):561–562

Rautio S, Hynynen P, Welling I, Hemmilä P, Usenius A, Närhi P (2007) Modelling of airborne dust emissions in CNC MDF milling. Holz Roh- Werkst 65(5):335–341

Reisz L, Magoss E (2013) Particle size distribution for different wood species and woodworking operation. Woodworking industry (1):38–45

Rekhadevi PV, Mahboob M, Rahman MF, Grover P (2008) Genetic damage in wood dust-exposed workers. Mutagenesis 24(1):59–65

Shamssain MH (1992) Pulmonary function and symptoms in workers exposed to wood dust. Thorax 47(2):84–87

Sitkei G (1994) A faipari műveletek elmélete (Theory of Wood Processing). Mezőgazdasági Szaktudás Kiadó Kft, Budapest, p 356

Teschke K, Hertzman C, Morrison B (1994) Level and distribution of employee exposures to total and respirable wood dust in two Canadian sawmills. Am Ind Hyg Assoc J 55(3):245–250

Timbrell V (1954) The terminal velocity and size of airborne dust particles. Br J Appl Phys 5(S3):S86

Wheatley GA (1951) Investigations on insecticidal dusts. First Report of the National Vegetable Research Station, Wellesbourne, pp 27–34

Whitehead LW, Ashikaga T, Vacek P (1981) Pulmonary function status of workers exposed to hardwood or pine dust. Am Ind Hyg Assoc J 42(3):178–186

Wu DW, Liu CR (1985) An analytical model of cutting dynamics. Part 1: Model building. ASME J Engg Industry 107(2):107–111

Zhang J, Shao Y, Huang N (2014) Measurements of dust deposition velocity in a wind-tunnel experiment. Atmos Chem Phys 14(17):8869–8882

Zhou C, Su J, Chen H, Shi Z (2021) Terminal velocity and drag coefficient models for disc-shaped particles based on the imaging experiment. Powder Technology, p 117062